1. Boumediene BENABDALLAH SEREIR[1], 2. Radhawane SADOUNI[2], 3. Ahmed TAHOUR[3], 4. Habib HAMDAOUI[4], 5. Salim DJERIOU[5]

LSTE Laboratory, University Mustapha Stambouli of Mascara, Algeria (1),
Materials, Energy Systems Technology and Environment Laboratory, Université de Ghardaia, Algeria (2),
Department of Electrical Engineering, ESSA of Tlemcen, Algeria (3),
ICEPS Laboratory, Department of Electrical, University of Djillali Liabes Sidi Bel Abbes, Algeria (4),
Faculty of Sciences and Technologies, University of M'sila, Algeria (5)

doi:10.15199/48.2022.05.16

Fuzzy Direct Field Oriented Control of a Double Stator Induction Motor (DSIM) with an MRAS Observer Dedicated to Photovoltaic Pumping System

Abstract *This paper presents the Direct Field Oriented Control (DFOC) scheme based on fuzzy logic speed controller without mechanical sensor (MRAS Observer) for a Double Stator Induction Motor fed by a two Pulse Width Modulation (PWM) voltage source inverters, by means of a photovoltaic solar panel using a maximum power point tracking (MPPT) control, dedicated to solar water pumping system (SWPS). So far several types of motors are used for solar water pumping systems and to the authors best knowledge; this is the first attempt to apply DSIM with this proposed control method to such a system. The simulation results show that the direct field oriented control with fuzzy controller and MRAS observer, provides good dynamic performances and presents a great robustness and efficiency*

Streszczenie. *W artykule przedstawiono schemat Direct Field Oriented Control (DFOC) oparty na regulatorze prędkości z logiką rozmytą bez czujnika mechanicznego (MRAS Observer) dla silnika indukcyjnego z podwójnym stojanem zasilanego z dwóch falowników napięcia z modulacją szerokości impulsu (PWM), za pomocą fotowoltaiki panel słoneczny wykorzystujący sterowanie śledzeniem maksymalnego punktu mocy (MPPT), dedykowany do słonecznego systemu pompowania wody (SWPS). Jak dotąd, według najlepszej wiedzy autorów, w solarnych systemach pompowania wody stosowanych jest kilka typów silników; jest to pierwsza próba zastosowania DSIM z tą proponowaną metodą sterowania do takiego systemu. Wyniki symulacji pokazują, że bezpośrednie sterowanie zorientowane na pole z kontrolerem rozmytym i obserwatorem MRAS zapewnia dobre osiągi dynamiczne i charakteryzuje się dużą wytrzymałością i wydajnością* (***Rozmyte bezpośrednie sterowanie zorientowane na pole silnika indukcyjnego z podwójnym stojanem (DSIM) z obserwatorem MRAS przeznaczonym do fotowoltaicznego układu pompowego***)

Keywords: Double Stator Induction Motor, Direct Field Oriented Control, Fuzzy Logic Controller, Photovoltaic Generator, MPPT,
Słowa kluczowe: silnik indukcyjny z podwójnym stojanem, sterowanie rozmyte, ogniwo fotowoltaiczne

Introduction

The power rating of an AC drive system can be increased by using high phase order drive system (multiphase machine) which has more than three phases in the stator of the machine. High phase order drive systems possess several advantages over conventional three-phase drives, such as reducing the amplitude and increasing the frequency of torque pulsation, reducing the rotor harmonic currents, reducing the current per phase without increasing the voltage per phase, and lowering the DC-Link current harmonics and high reliability. Otherwise, losing of one or more phases in a high phase order drive system does not prevent the machine from starting and running [1].

Photovoltaic energy is a renewable energy source, inexhaustible and non-polluting. To be used for different applications and to meet the economic constraints, the design and implementation of PV systems are necessary and currently facing many problems. The PV system must be made robust, reliable and with high efficiency [2, 3].

The most popular application of the photovoltaic energy is stand-alone water pumping system driven by electrical motors. Indeed, it is the best adopted energy source to supply drinking and irrigating water in remote regions which economically cannot benefit from the national grid connection [4]. In such applications, high efficiency and reliability are required. Many types of motors are available for use in SWPS (solar water pumping system).

At early stage brushed DC motors were extensively used to drive water pumps [5, 6] and continue to be used [7, 8]. After that it has been turned out that the reliability of SWPS can be improved by using brushless DC motors [9] and switched reluctance motors [10]. For high power and/or when high reliability SWPS is required, AC induction motors seem to be the adequate alternative [11, 12] compared to the aforementioned motors. The present paper introduces the use of DSIM that is a common type of multiphase machine.

The main difficulty in the asynchronous machine control resides in the fact that complex coupling exists between the field and the torque. The major disadvantage of conventional algorithms of regulation such as PID controllers is the sensitivity to the motor parametric variation [13]. For the control, the major problem is the need for using a mechanical sensor. This imposes an additional cost and increases the complexity of the assembly [14]. To eliminate all these problems and difficulties, the vector control using fuzzy logic controller without using a mechanical sensor is proposed.

Design of proposed system

Figure 1 shows the proposed architecture of the SWPS. This section presents the mathematical model of each component constituting the end-to-end power conversion chain.

Photovoltaic generator and boost converter

Photovoltaic generator can supply the maximum power to the load, the power of the panel generator must be adjusted to the appropriate value by regulating the voltage of PV panel to the MPP operating voltage. The technique conventionally employed is to use an adaptation stage between the PVG and the load. In this paper we use a boost converter, which is mostly used in photovoltaic applications, especially in photovoltaic pumping system. This converter is important in PV system since it has the ability of regulating the output voltage. The output voltage can be controlled to be greater than the input voltage by varying the duty cycle control. The control that makes the PVG's output power as close as possible to Pmax is known as MPPT. MPPT stands for maximum power point tracking which is essential for optimizing the PVG operation and the whole system performance. Improving the performances of PV-fed systems in general is very important issue for scientific community as well as for industrial investors as long as the central problem of the PVG is the low efficiency. There are several methods that have been widely used to track the MPP such as the P&O technique known for its speed, accuracy and quality of sizes obtained by the proper choice of the step increment, that it's used in this paper [15, 16, 17].

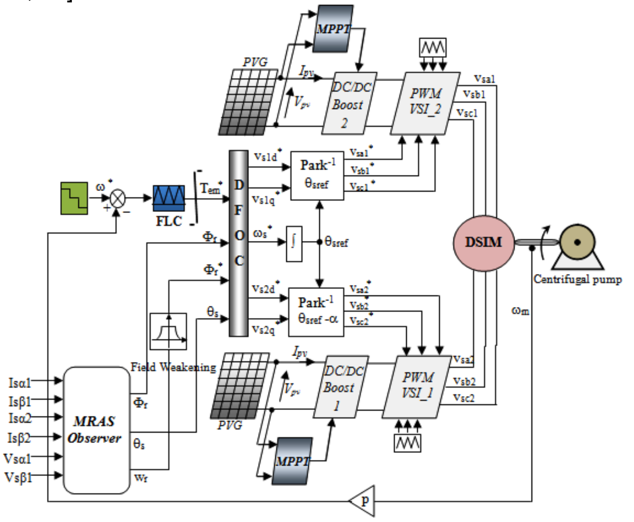

Fig.1. Schematic diagram of proposed solar water pumping system

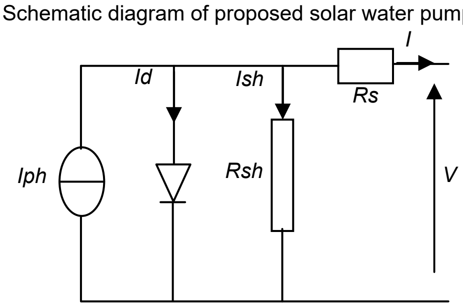

Fig.2. Equivalent circuit of a PV module

(1) $$I = I_{ph} - I_d - I_{sh}$$

(2) $$I_d = I_0\left(\exp\left(\frac{q(V + R_s I)}{kAT}\right) - 1\right)$$

(3) $$I_{sh} = \frac{V + R_s I}{R_{sh}}$$

where: Iph: is the photocurrent; Id: is the junction diode current; I0: is the reverse saturation current; Rs: is the series resistance; Rsh: is the parallel resistance; A: is the diode factor; k: is the Boltzmann's constant; T: is the cell temperature; q: is the electron charge

Voltage source inverter

The three-phase inverter is one of the structures used in energy conversion for powering AC loads; it consists of three independent legs. Each one includes two switches which are complementary and controlled by the Pulse Width Modulation (PWM) circuit [18]. The induction motor stator voltages (V_{sa}, V_{sb}, V_{sc}) are expressed in terms of states of the upper switches as below:

(4) $$\begin{bmatrix} V_{sa} \\ V_{sb} \\ V_{sc} \end{bmatrix} = \frac{Upv}{3}\begin{bmatrix} 2 & -1 & -1 \\ -1 & 2 & -1 \\ -1 & -1 & 2 \end{bmatrix}\begin{bmatrix} f_{11} \\ f_{12} \\ f_{13} \end{bmatrix}$$

Upv: The photovoltaic voltage.
f11, f12 and f13 are the controller signals applied to the inverter's three upper switches.

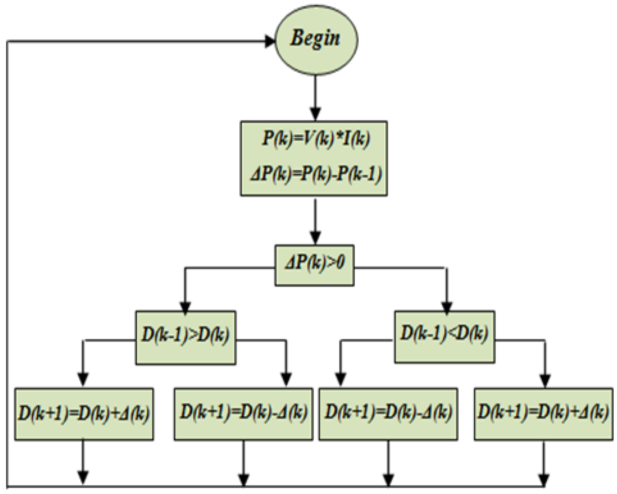

Fig.3. P&O algorithm

Modeling of the DSIM

A schematic of the stator and rotor windings for a Double Stator Induction Motor is given in Figure 4. The six stator phases are divided into two wyes-connected three phase sets labeled A_{s1}, B_{s1}, C_{s1} and A_{s2}, B_{s2}, C_{s2} whose magnetic axes are displaced by an angle α=30°. The windings of each three phase set are uniformly distributed and have axes that are displaced 120° apart. The three phase rotor windings A_r, B_r, C_r are also sinusoidally distributed and have axes that are displaced apart by 120° [19].

The following assumptions are made: [20, 21]:
- Motor windings are sinusoidally distributed;
- The two stars have same parameters;
- The magnetic saturation, the mutual leakage inductances and the core losses are negligible;
- Flux path is linear.

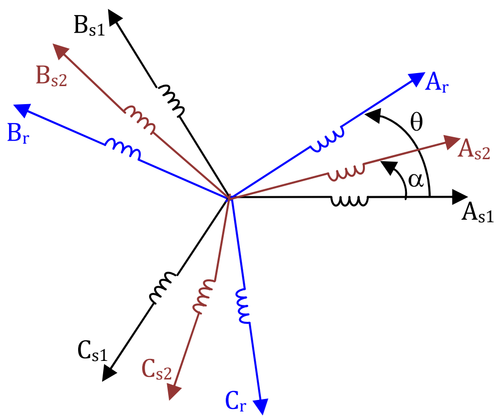

Fig.4. Windings of the double stator induction motor

The voltage equations of the DSIM are as follow [22]:

(5)
$$[V_{s1}]=\begin{bmatrix}V_{sa1}\\V_{sb1}\\V_{sc1}\end{bmatrix}=[R_{s1}][I_{s1}]+\frac{d}{dt}[\Phi_{s1}]$$

$$[V_{s2}]=\begin{bmatrix}V_{sa2}\\V_{sb2}\\V_{sc2}\end{bmatrix}=[R_{s2}][I_{s2}]+\frac{d}{dt}\left[\Phi_{s2}\right]$$

$$[0]=\begin{bmatrix}V_{ra}\\V_{rb}\\V_{rc}\end{bmatrix}=[Rr][Ir]+\frac{d}{dt}[\Phi_r]$$

(6)
$$[R_{s1}]=\begin{bmatrix}R_{s1}&0&0\\0&R_{s1}&0\\0&0&R_{s1}\end{bmatrix}$$

$$[R_{s2}]=\begin{bmatrix}R_{s2}&0&0\\0&R_{s2}&0\\0&0&R_{s2}\end{bmatrix}$$

$$[R_r]=\begin{bmatrix}R_r&0&0\\0&R_r&0\\0&0&R_r\end{bmatrix}$$

Where:
$R_{sa1} = R_{sb1} = R_{sc1} = R_{s1}$: Star resistance 1.
$R_{sa2} = R_{sb2} = R_{sc2} = R_{s2}$: Star resistance 2.
$R_{ra} = R_{rb} = R_{rc} = R_r$: Rotor resistance.

(7)
$$[I_{s1}]=\begin{bmatrix}I_{sa1}\\I_{sb1}\\I_{sc1}\end{bmatrix};\ [I_{s2}]=\begin{bmatrix}I_{sa2}\\I_{sb2}\\I_{sc2}\end{bmatrix};\ [I_r]=\begin{bmatrix}I_{ra}\\I_{rb}\\I_{rc}\end{bmatrix}$$

(8)
$$[\Phi_{s1}]=\begin{bmatrix}\Phi_{sa1}\\\Phi_{sb1}\\\Phi_{sc1}\end{bmatrix};[\Phi_{s2}]=\begin{bmatrix}\Phi_{sa2}\\\Phi_{sb2}\\\Phi_{sc2}\end{bmatrix};[\Phi_r]=\begin{bmatrix}\Phi_{ra}\\\Phi_{rb}\\\Phi_{rc}\end{bmatrix}$$

The expressions for star and rotor flux are [22]:

(9)
$$\begin{bmatrix}[\Phi_{s1}]\\ [\Phi_{s2}]\\ [\Phi_r]\end{bmatrix}=\begin{bmatrix}[L_{s1s1}]&[L_{s1s2}]&[L_{s1r}]\\ [L_{s2s1}]&[L_{s2s2}]&[L_{s2r}]\\ [L_{rs1}]&[L_{rs2}]&[L_{rr}]\end{bmatrix}.\begin{bmatrix}[I_{s1}]\\ [I_{s2}]\\ [I_r]\end{bmatrix}$$

where: [Ls1s1]: Inductance matrix of the star 1; [Ls2s2]: Inductance matrix of the star 2; [Lrr]: Inductance matrix of the rotor; [Ls1s2]: Mutual inductance matrix between star 1 and star 2; [Ls2s1]: Mutual inductance matrix between star 2 and star 1; [Ls1r]: Mutual inductance matrix between star 1 and rotor; [Ls2r]: Mutual inductance matrix between star 2 and rotor; [Lrs1]: Mutual inductance matrix between rotor and star 1; [Lrs2]: Mutual inductance matrix between rotor and star 2.

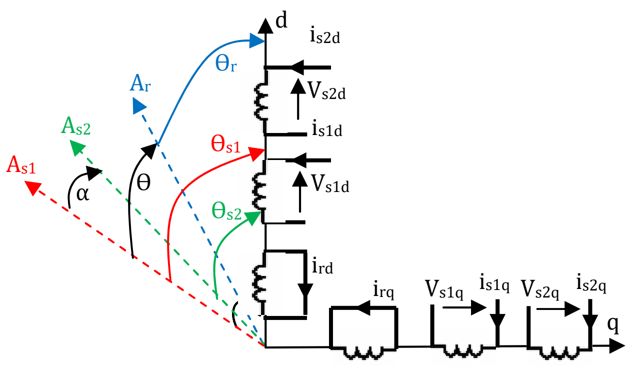

Fig.5. Representation of DSIM in the Park frame

The expression of the electromagnetic torque is then as follows [22, 23, 24]:

(10)
$$Tem=\left(\frac{p}{2}\right).\left([I_{s1}]\frac{d}{d\theta}[L_{s1r}].[I_r]+[I_{s2}]\frac{d}{d\theta}[L_{s2r}][I_r]\right)$$

The Park model of the DSIM in the references frame at the rotating field (d, q), is defined by the following equations system (11) [25].
The Figure 5 represents the model of the DSIM in the Park frame.

(11)
$$\begin{aligned}
V_{s1d} &= R_{s1}I_{s1d}+\frac{d}{dt}\Phi_{s1d}-\omega_s\Phi_{s1q}\\
V_{s1q} &= R_{s1}I_{s1q}+\frac{d}{dt}\Phi_{s1q}+\omega_s\Phi_{s1d}\\
V_{s2d} &= R_{s2}I_{s2d}+\frac{d}{dt}\Phi_{s2d}-\omega_s\Phi_{s2q}\\
V_{s2q} &= R_{s2}I_{s2q}+\frac{d}{dt}\Phi_{s2q}+\omega_s\Phi_{s2d}\\
0 &= R_rI_{rd}+\frac{d\Phi_{rd}}{dt}-\omega_{sr}\Phi_{rq}\\
0 &= R_rI_{rq}+\frac{d\Phi_{rq}}{dt}+\omega_{sr}\Phi_{rd}
\end{aligned}$$

Where:

(12)
$$\begin{aligned}
\Phi_{s1d} &= L_{s1}I_{s1d}+L_m(I_{s1d}+I_{s2d}+I_{rd})\\
\Phi_{s1q} &= L_{s1}I_{s1q}+L_m(I_{s1q}+I_{s2q}+I_{rq})\\
\Phi_{s2d} &= L_{s2}I_{s2d}+L_m(I_{s1d}+I_{s2d}+I_{rd})\\
\Phi_{s2q} &= L_{s2}I_{s2q}+L_m(I_{s1q}+I_{s2q}+I_{rq})\\
\Phi_{rd} &= L_rI_{rd}+L_m(I_{s1d}+I_{s2d}+I_{rd})\\
\Phi_{rq} &= L_rI_{rq}+L_m(I_{s1q}+I_{s2q}+I_{rq})
\end{aligned}$$

L_m: Cyclic mutual inductance between star 1, star 2 and rotor.
The mechanical equation is given by:

(13)
$$J\frac{d\Omega}{dt}=T_{em}-T_L-F_r\Omega$$

With:

(14)
$$Tem=p\frac{L_m}{L_r+L_m}\left[\Phi_{rd}(I_{s1q}+I_{s2q})-\Phi_{rq}(I_{s1d}+I_{s2d})\right]$$

Modeling of the centrifugal pump

Depending upon the intended application, the pump of the SWPS can be selected to be surface, submersible or floating pump. In this paper, we used the centrifugal pump. Centrifugal pumps are economical from shallow to medium lifts with large flow rates. Axial flow pumps are dynamic pumps that use the propeller to create a lift action of the fluid in the pipe. These pumps used in wet-pit drainage, storm water applications, and low pressure irrigation [17].
Each centrifugal pump applies a load torque proportional to the square of the rotor speed [26, 27].

(15)
$$T_L=K_p\Omega_r^2$$

Where K_p is the proportionality constant and it is given by:

(16)
$$K_p=P_{np}/\Omega_{rn}^3$$

The water rate and pressure of the pump depend on the available mechanical power at the rotating impeller and the total head. The determination of the pump's output parameters can be simplified using affinity laws [17] which require only pump ratings and actual input parameters; rotor speed and torque.

$$(17)\quad \begin{cases} Q' = (\Omega_r / \Omega_{rn}).Q \\ H' = (\Omega_r / \Omega_{rn})^2.H \\ P' = (\Omega_r / \Omega_{rn})^3.P \end{cases}$$

Where H, Q and P are the rated parameters of the pump at speed Ω_{rn}. H', Q' and P' are the parameters of pump at speed Ω_r different than the rated speed.

Direct field oriented control of a DSIM

For the direct vector control, the rotor flux magnitude will be controlled by feedback. For this purpose, a field rotor estimator is achieved from currents measurements (ids and iqs) and the rotor currents pulsation (wr). The application of the field oriented control consists on the orientation of the rotor flux vector along the "d" axis which can be expressed by considering (Øqr=0 and Ødr=Ør*). The finals expressions of the electromagnetic torque and slip speed are [28]:

$$(18)\quad T_{em} = p\frac{L_m}{L_m + L_r}\overset{*}{\Phi}_r(\overset{*}{I}_{s1q} + \overset{*}{I}_{s2q})$$

$$(19)\quad \overset{*}{w}_{sr} = \frac{R_r L_m}{(L_m + L_r)\overset{*}{\Phi}_r}(\overset{*}{I}_{s1q} + \overset{*}{I}_{s2q})$$

The stators voltage equations are:

$$(20)\quad \begin{aligned} \overset{*}{V}_{s1d} &= R_{s1}I_{s1d} + L_{s1}\frac{d}{dt}I_{s1d} - \overset{*}{\omega}_s(L_{s1}I_{s1q} + T_r\overset{*}{\Phi}_r\overset{*}{w}_{sr}) \\ \overset{*}{V}_{s1q} &= R_{s1}I_{s1q} + L_{s1}\frac{d}{dt}I_{s1q} + \overset{*}{\omega}_s(L_{s1}I_{s1d} + \overset{*}{\Phi}_r) \\ \overset{*}{V}_{s2d} &= R_{s2}I_{s2d} + L_{s2}\frac{d}{dt}I_{s2d} - \overset{*}{\omega}_s(L_{s2}I_{s2q} + T_r\overset{*}{\Phi}_r\overset{*}{w}_{sr}) \\ \overset{*}{V}_{s2q} &= R_{s2}I_{s2q} + L_{s2}\frac{d}{dt}I_{s2q} + \overset{*}{\omega}_s(L_{s2}I_{s2d} + \overset{*}{\Phi}_r) \end{aligned}$$

The torque expression shows that the reference fluxes and stator currents in quadrate are not perfectly independent, for this, it is necessary to decouple torque and flux control of this machine by introducing new variables [19, 28]:

$$(21)\quad \begin{aligned} V_{s1d} &= R_{s1}I_{s1d} + L_{s1}\frac{d}{dt}I_{s1d} \\ V_{s1q} &= R_{s1}I_{s1q} + L_{s1}\frac{d}{dt}I_{s1q} \\ V_{s2d} &= R_{s2}I_{s2d} + L_{s2}\frac{d}{dt}I_{s2d} \\ V_{s2q} &= R_{s2}I_{s2q} + L_{s2}\frac{d}{dt}I_{s2q} \end{aligned}$$

The equation system (21) shows that stator voltages (V_{s1d}, V_{s1q}, V_{s2d}, V_{s2q}) are directly related to stator currents (I_{s1d}, I_{s1q}, I_{s2d}, I_{s2q}). To compensate the error introduced at decoupling time, the voltage references (V_{s1d}^*, V_{s2d}^*, V_{s1q}^*, V_{s2q}^*) at constant flux are given by:

$$(22)\quad \begin{aligned} V_{s1d}^* &= V_{s1d} - V_{s1dc} \\ V_{s1q}^* &= V_{s1q} + V_{s1qc} \\ V_{s2d}^* &= V_{s2d} - V_{s2dc} \\ V_{s2q}^* &= V_{s2q} + V_{s2qc} \end{aligned}$$

With:

$$(23)\quad \begin{aligned} V_{s1dc} &= \overset{*}{\omega}_s(L_{s1}I_{s1q} + T_r\overset{*}{\Phi}_r\overset{*}{w}_{sr}) \\ V_{s1qc} &= \overset{*}{\omega}_s(L_{s1}I_{s1d} + \overset{*}{\Phi}_r) \\ V_{s2dc} &= \overset{*}{\omega}_s(L_{s2}I_{s2q} + T_r\overset{*}{\Phi}_r\overset{*}{w}_{sr}) \\ V_{s2qc} &= \overset{*}{\omega}_s(L_{s2}I_{s2d} + \overset{*}{\Phi}_r) \end{aligned}$$

For a perfect decoupling, we add stator currents regulation loops (I_{s1d}, I_{s1q}, I_{s2d}, I_{s2q}) and we obtain at their output stator voltages (V_{s1d}, V_{s1q}, V_{s2d}, V_{s2q}). The decoupling bloc scheme in voltage modified (Modified Field Oriented Control) is given in Figure 6.

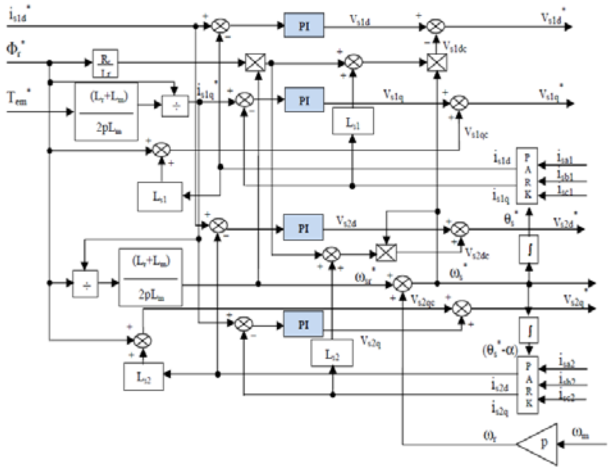

Fig.6. Decoupling bloc in voltage

Fuzzy logic control

Traditional control design methods use mathematical models of a system and its inputs to design controllers. Fuzzy logic control uses Fuzzy sets and Fuzzy inference to derive control laws in which no precise model of the plants is available, and most of the expertise is available only in qualitative form. The basic idea of Fuzzy Logic control is to make use of expert knowledge to build a rule based controllers [28]. The Fuzzy control processing, in general, is typically divided into the following three stages: Fuzzification, inference engine plus rules base and Defuzzification, as shown in figure 7. The Fuzzification process means that real world variables are translated into Fuzzy values using fuzzy sets (fuzzy set membership). The control algorithm is coded using Fuzzy statements in the block containing the knowledge base by taking into account the control objectives and the system behavior. The second stage includes the rules base and the Fuzzy inference engine. The control objectives taking into account the system behavior are coded under the form of rules "IF THEN". The way it is processed the fuzzy rule is decided by the inference engine. The results of the Fuzzy computations are translated in terms of real values for the Fuzzy control action by the Defuzzification block [28].

There is no systematic methodology to select the FLC system parameters, such as the number fuzzy sets, the shape of membership functions μ(x), and the universe of discourse of input and output variables, etc. The greater is the number of linguistic values the more processing time it requires and better accuracy will be. In this paper, following our experience in using fuzzy logic, we have chosen a Fuzzy Logic Controller with five fuzzy values (Negative Large, Negative, Zero, Positive, Positive Large) for each variable of the controller [3].

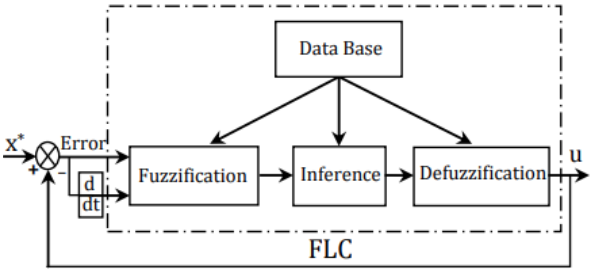

Fig.7. Fuzzy controller structure

The middle fuzzy values have triangle membership functions whereas the extreme values have rectangular shape. The figure 8 shows the parameters of each variable x (x can be e, ë or du) used in the FL Controller. The inputs to the fuzzification process are the speed error and its derivative [3].

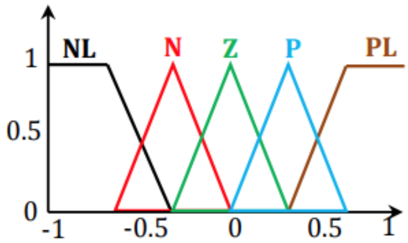

Fig.8. Universe of discourse, fuzzy values and their shape forms

Table 1 represent a table of rules for two linguistic variables of input; the speed error «e» and its variation «de» and the output variable «du».

Table 1. Rules bases for speed control

du		***e***				
		NL	N	Z	P	PL
de	NL	NL	NL	NL	N	Z
	N	NL	N	N	Z	P
	Z	NL	N	Z	P	PL
	P	N	Z	P	P	PL
	PL	Z	P	PL	PL	PL

MRAS Observer

The adaptive system using a reference model (MRAS) is composed of two flux estimators. The first is called the reference model (usually it is a current model). The second is called the adjustable model [29] (usually a voltage model) (Figure 9). The adaptive model of observer is described by equation (24):

$$(24)\quad \begin{cases} \dfrac{d\hat{\phi}_{r\alpha i}}{dt} = \dfrac{L_m}{T_r}(i_{\alpha s1} + i_{\beta s1}) - \dfrac{1}{T_r}\hat{\phi}_{r\alpha i} - \omega_r \hat{\phi}_{\beta ri} \\ \dfrac{d\hat{\phi}_{r\beta i}}{dt} = \dfrac{L_m}{T_r}(i_{\alpha s1} + i_{\beta s1}) - \dfrac{1}{T_r}\hat{\phi}_{r\beta i} - \omega_r \hat{\phi}_{\beta ri} \end{cases}$$

And the reference model is given [30] by equation (25):

$$(25)\quad \frac{d\hat{\phi}_{r\alpha v}}{dt} = \frac{L_r + L_m}{L_m}\left(v_{\alpha s1} - R_s i_{\alpha s1} - \sigma(L_s + L_m)\frac{di_{\alpha s1}}{dt} - \frac{L_m L_r}{L_m + L_r}\frac{di_{\alpha s2}}{dt}\right)$$

$$\frac{d\hat{\phi}_{r\beta v}}{dt} = \frac{L_r + L_m}{L_m}\left(v_{\beta s1} - R_s i_{\beta s1} - \sigma(L_s + L_m)\frac{di_{\beta s1}}{dt} - \frac{L_m L_r}{L_m + L_r}\frac{di_{\beta s2}}{dt}\right)$$

The error for the corrector is calculated according to the cross product [31, 32, 33]:

$$(26)\quad \varepsilon = \hat{\phi}_{\alpha ri} \cdot \phi_{r\beta v} - \hat{\phi}_{\alpha rv} \cdot \phi_{r\beta i}$$

The law of adaptation is given by the following expression [34]:

$$(27)\quad \hat{\omega}_r = \varepsilon\left(k_p + \frac{k_i}{s}\right)$$

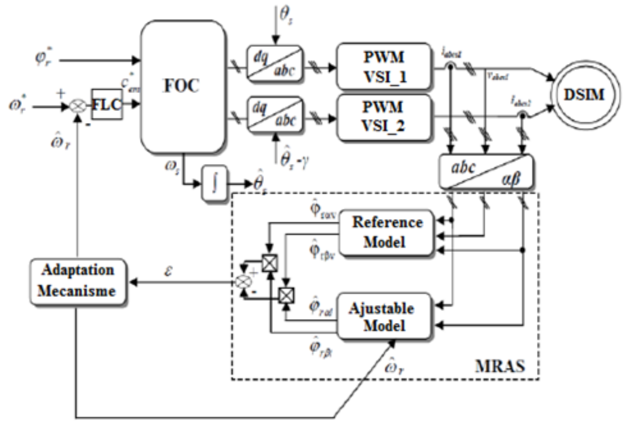

Fig.9. Fuzzy speed sensorless control of field-oriented DSIM with MRAS observer

Table 2. Dual Stator Induction Machine parameters

P_n [kw]	4.5	R_r [Ω]	2 .12	J [kg.m^2]	0.062
V_n [V]	220	L_{s1} [H]	0.022	f_r [Nms/r]	0.001
I_n [A]	6.5	L_{s2} [H]	0.022	f [Hz]	50
R_{s1} [Ω]	3.72	L_r [H]	0.006	p	1
R_{s2} [Ω]	3.72	L_m [H]	0.367	Cos φ	0.8

Table 3. Pump parameters

Q=4.7(m^3/h)	H=180(m)
N=2950(r/min)	

Table 4. Photovoltaic model Characteristics

Parameter	Value
Maximum Power (Pmax)	150W
Voltage at Pmax (Vmp)	34.5V
Current at Pmax (Imp)	4.35A
Open-circuit voltage (Voc)	43.5
Short-circuit current (Isc)	4.75A
Temperature coefficient of Voc	-160 ± 20 mV/°C
Temperature coefficient of Isc	0.065 ± 0.015 %/°C
Temperature coefficient of power	-0.5 ± 0.05 %/°C

Simulation results and discussion

In order to demonstrate the effectiveness of the proposed architecture applied to the photovoltaic water-pumping system using fuzzy indirect field oriented control, a simulation framework has been carried out. The proposed design scheme shown in figure 1 is implemented using Matlab/Simulink software where parameters of all SWPS components are given in the appendix.

We chose a constant irradiation E, equal to 1000W/m^2, the simulation results using Matlab/Simulink are given in the following figures.

The estimated speed tracks the real and the reference speed (300, 150 and 100 rad/s) with no steady-state error. The load torque disturbance is rejected in the speed response rapidly. The motor develops an electromagnetic torque to compensate the load torque of centrifugal pump and the stator current decrease with the decrease of the load torque, it keeps a sinusoidal form and it has very good dynamic. The observed rotor field reaches his measured field without overtaking. The flow rate and the height of the centrifugal pump are very close to their optimal values.

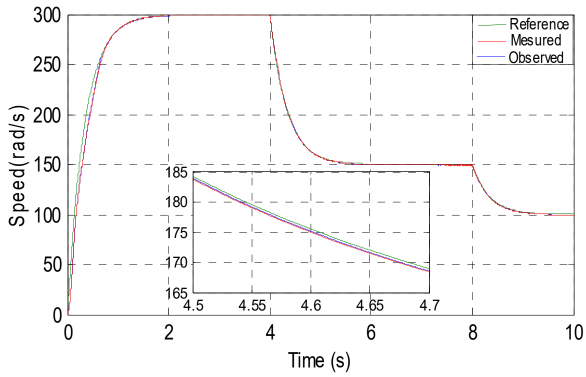

Fig.10. Rotor speed and its reference

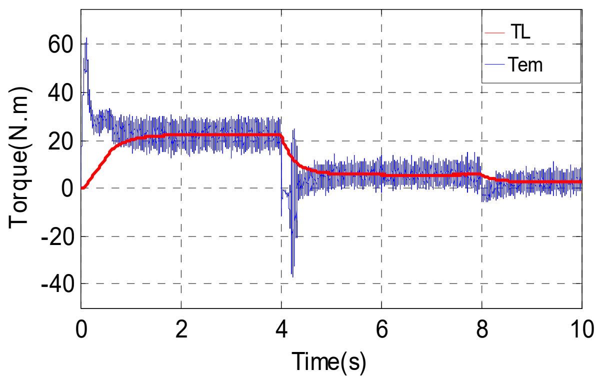

Fig.11. Electromagnetic and load torque

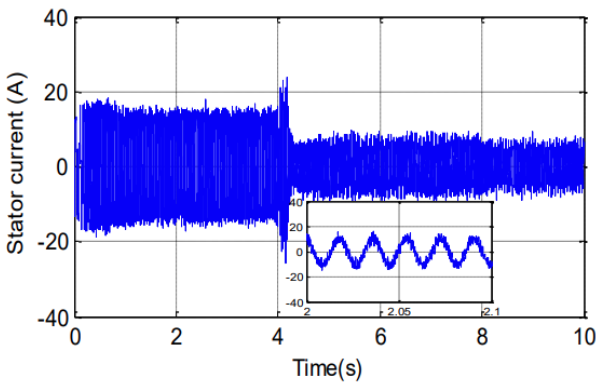

Fig.12. The stator current

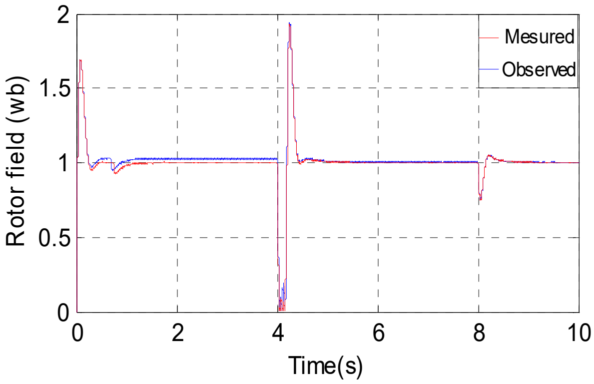

Fig.13. Measured and observed rotor field

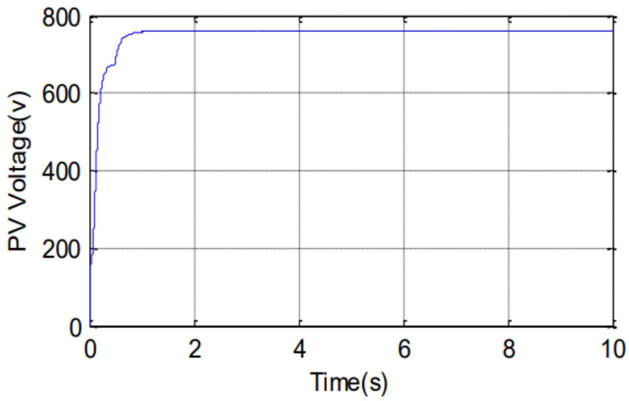

Fig.14. The photovoltaic voltage

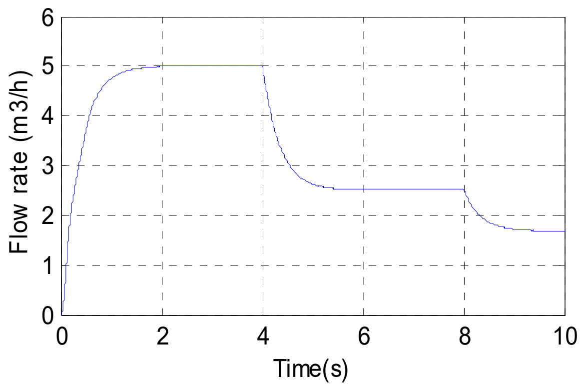

Fig.15. Evolution of the flow rate

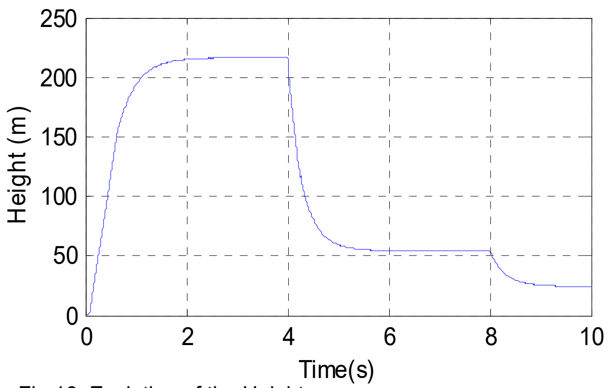

Fig.16. Evolution of the Height

Conclusion

In this paper a fuzzy speed sensorless direct vector control of double stator induction motor using MRAS observer dedicated to solar water pumping system is presented. We proposed in this architecture the use of DSIM with global optimization using Perturb and Observe MPPT algorithm. Direct field oriented control scheme with MRAS observer is used to decouple the nonlinear structure of the DSIM and fuzzy sets based controller to handle the uncertainties related to the modeling of AC double stator induction motor. According to the simulation results, we can conclude that the proposed scheme shows good static and dynamic performances.

Acknowledgements

We gratefully thank the Directorate General for Scientific Research and Technological Development (DGSRTD) affiliated with the Ministry of Higher Education and Scientific Research in Algeria, for his support of our laboratory.

Authors: *Ph.D. Boumediene BENABDALLAH SEREIR, LSTE Laboratory, University Mustapha Stambouli of Mascara, P O Box: 305, road of Mamounia, Mascara 29000, Algeria, email : benabdallahboumediene@yahoo.fr*
Radhwane Sadouni – Materials, Energy Systems Technology and Environment Laboratory, Faculty of Sciences and Technologies, Université de Ghardaia, Algeria, email: sadouni.radhwane@univ-ghardaia.dz ; redouanesadouni@gmail.com
Ahmed Tahour – Department of Electrical Engineering, ESSA of Tlemcen, Algeria, email: Tahourahmed@yahoo.fr
Habib hamdaoui Department of Electrical, University of Djillali LiabesSidi Bel Abbes, Algeria, email: hamdaoui_h@outlook.fr
Salim Djeriou – Faculty of Sciences and Technologies, University of M'sila, Algeria, email: salimjr28@yahoo.fr

REFERENCES

[1] R. Sadouni, A. Meroufel, S. Djriou, "Study and Simulation of Direct Torque Control (DTC) for a Six Phase Induction Machine (SPIM)". International journal of energy, Issue 2, Vol. 7, 2013. pp: 31-37.
[2] R. Sadouni, A. Meroufel, S. Djriou, A. Kheldoun, A "Fuzzy Sliding Mode Robust Control for a Field Oriented Dual Star Induction Machine Fed by Photovoltaic Power Supply with MPPT Algorithm". The Mediterranean Journal of Measurement and Control, Issue 4, Vol. 12, 2016. pp: 654-663.
[3] S. Djeriou, A. Kheldoun, R. Sadouni, "Fuzzy indirect field oriented control of a dual star induction motor water pumping system fed by photovoltaic generator". Engineering Intelligent Systems, Issue 2, Vol. 23, 2015. pp: 63-76.
[4] K. Meah, S. Fletcher, S. Ula, "Solar photovoltaic water pumping for remote locations". Renewable and Sustainable Energy Reviews, 12, 2008. 472–487.
[5] M. Akbaba, I. Qamber, A. Kamal, "Matching of separately excited dc motors to photovoltaic generators for maximum power output". Solar Energy, 63, 1989. 375–385.
[6] J. Appelbum, "Starting and steady state characteristic of DC motor powered by solar cell generator". IEEE Trans. on Energy Conversion, 1, 1986. 17–27.
[7] M. Kolhe, J.C. Joshi, D.P. Kothari, "Performance Analysis of a Directly Coupled Photovoltaic Water- Pumping System". Trans. on Energy Conversion 19, (2004). 613–618.
[8] Z. Abidin Firatoglu, B. Yesilata, "New approaches on the optimization of Directly Coupled photovoltaic Water- Pumping System". Solar Energy 77, (2004). 81–93.
[9] A. Terki, A. Moussi, A. Betka, N. Terki, "An improved efficiency of fuzzy logic control of PMBLDC for PV pumping system". Applied Mathematical Modelling, 36, (2012). 934–944.
[10] M. Nabil, S.M. Allam, E.M. Rashed, "Performance improvement of a photovoltaic pumping system using synchronous reluctance motor". Elect. Pow. Comp and Systems, 41, 2013. 447-464.
[11] C. Gopal, M. Mohanraj, P. Chandramohan, P. Chandrasekar, "Renewable energy source water pumping systems_ A literature review". Renewable and Sustainable Energy Reviews, 25, 2013. 351–370.
[12] J.V.M. Caracas, G.C. Farias, L.F.M. Teixeira, L.A.S. Ribeiro,"Implementation of a High-efficiency, High-lifetime, and low-cost Converter for an Autonomous Photovoltaic Water Pumping system". IEEE, Trans on Industry Applications, Vol. 50, No. 1, 2014.
[13] R. Sadouni, A. Meroufel, "Indirect Rotor Field-oriented Control (IRFOC) of a Dual Star Induction Machine (DSIM) Using a Fuzzy Controller". Acta Polytechnica Hungarica, Issue 4, Vol. 9, 2012. pp: 177-192.
[14] M.H. Lazreg, A. Bentaallah, "Sensorless fuzzy sliding-mode control of the double-star induction motor using a sliding-mode observer". Elektrotehniški Vestnik 85(4): 169-176, 2018.
[15] C.S. Chin, P. Neelakantan, H.P. Yoong, K.T.K. Teo, "Fuzzy Logic Based MPPT for Photovoltaic Modules Influenced by Solar Irradiation and Cell Temperature". IEEE, 2011.
[16] S. Arezki, M. Boudour, "Simulation and Modeling of a Photovoltaic System Adapted by a MPPT control reaction, Application on a DSIM". 2010 IEEE International Energy Conference, IEEE, 2010.
[17] S. Djeriou, "Performance Improvement of Photovoltaic Pumping System". PhD Thesis, Institute of Electrical and Electronic Engineering. University of Boumerdes, 2018.
[18] G.K. Singh, K. Nam, S.K. Lim, "A simple indirect field-oriented control scheme for multiphase induction machine". IEEE Trans. Ind. Elect., vol. 52, no. 4, pp. 1177–1184, August 2005.
[19] R. Sadouni, A. Meroufel, "Performances comparative study of Field Oriented Control (FOC) and Direct Torque Control (DTC) of Dual Three Phase Induction Motor (DTPIM)". International Journal of Circuits, Systems and Signal Processing, Issue 2, Volume 6, 2012, pp: 163-170.
[20] P. Vidal, "Commande non-linéaire d'une machine asynchrone à double alimentation", Thèse de Doctorat de l'Institut National Polytechnique de Toulouse, France, Décembre 2004.
[21] R. Bojoi, M. Lazzari, F. Profumo, A. Tenconi, "Digital Field-Oriented Control for Dual Three-Phase Induction Motor Drives". IEEE Transactions On Industry Applications, Vol. 39, No.3, May/June 2003.
[22] E.M. Berkouk, S. Arezki, "Modélisation et Commande d'une Machine Asynchrone Double Etoile (MASDE) Alimentée par Deux Onduleurs à Cinq Niveaux à Structure NPC". Conférence national sur le génie électrique, CNGE, Tiaret, Algérie, 2004.
[23] A. Igoudjil, Y. Boudjema, "Etude du changeur de fréquence à cinq niveaux à cellules imbriquées. Application à la conduite de la machine Asynchrone à Double Etoile". Engineer memory, USTHB, Algiers, Algeria, 2006.
[24] D. Hadiouche, "Contribution à l'étude de la machine asynchrone double étoile modélisation, alimentation et structure". Thèse de doctorat, PhD thesis, Université Henri Poincaré, Nancy-1, France, 2001.
[25] Z. Chen, A.C. Williamson, "Simulation Study of a Double Three Phase Electric Machine". Proc. ICEM conf. on Electric Machine, Istanbul, Turkey, 1998.
[26] R. Kumar, B. Singh, A. Chandra, Al-haddad K, "Solar OV array water pumping using BLDC motor drive with boost-buck converter". Proceedings of the IEEE Energy Conversion Congress and Exposition ECCE; 2015. p. 5741-5748.
[27] M. Thierry, G. Christian, J. Charles, R. Benoît, "A simplified but accurate prevision method for along the sun PV pumping systems". Sol Energy 2008; 82 (11): 1009–1020.
[28] I. Eker, Y. Torun, "Fuzzy logic control to be conventional method". Energy Conversion and Management, 47, 377–394, 2006.
[29] G.C. Hwang, S.C. Lin, "A stability approach to fuzzy control design for non linear systems". Fuzzy Sets Syst., vol. 48, 279–287, 1992.
[30] T.S. Kwon, M.H. Shin, D.S. Hyun, "Speed sensorless stator flux-oriented control of induction motor in the field weakening region using Luenberger observer". IEEE Trans. on Power Electron., Vol. 20, No. 04, pp. 864–869, 2005.
[31] C. Schauder, "Adaptive Speed Identification for Vector Control of Induction Motors without Rotational Transducers". IEEE Transactions on Industry Applications Vol. 28 No. 5 1054-1061, 1992.
[32] I. Rouh, "Contribution à la commande sans capteur de la machine asynchrone". Thèse de Doctorat, Université de Henri Poincaré, Nancy, France, 2004.
[33] S. Maiti, C. Chakraborty, Y. Hori, M.C. Ta, "Model Reference Adaptive Controller-Based Rotor Resistance and Speed Estimation Techniques for Vector Controlled Induction Motor Drive Utilizing Reactive Power". IEEE Transactions on Industrial Electronics Vol. 55 No. 2, 594-601, 2008.
[34] V. Vasic, S.N. Vukosavic, E. Levi, "A Stator Resistance Estimation Scheme for Speed Sensorless Rotor Flux Oriented Induction Motor Drives". IEEE Transactions on Energy Conversion, Vol. 18 No. 4 476-483, 2003.